Performance Characteristics of a Reversible Immunosensor with a Heterobifunctional Enzyme Conjugate as Signal Generator

Se-Hwan Paek,[1] Willfried Schramm[2]

[1]Graduate School of Biotechnology, Korea University, Anam-Dong, Seoul 136-701, Republic of Korea; telephone: 82-415-60-1414; fax: 82-415-864-2665; e-mail: shpaek@tiger.korea.ac.kr
[2]Saliva Diagnostic Systems, Inc., 11719 NE 95th Street, Vancouver, Washington 98682

Received 21 August 1996; accepted 1 March 1997

Abstract: Factors that control the performance of a reversible immunosensor with an analyte (progesterone)–enzyme (horseradish peroxidase) conjugate as signal generator have been investigated. The conjugate is used in conjunction with two antibodies, which are specific to progesterone and to horseradish peroxidase, immobilized on two spatially separated polypropylene mesh discs. The conjugate and two antibodies are confined to an internal compartment of a microdialyzer by a semipermeable membrane. The small analyte from an external medium permeates across the membrane into the internal compartment where the analyte concentration determines the relative amounts of the bound conjugate on the two solid surfaces. By measuring two signals from the conjugate bound at two separate sites, we experimentally obtained time–response curves to a concentration pulse of the external analyte. A mathematical (kinetic) model describing the sensor system was developed and used for the determination of rate-limiting factors. In semicontinuous monitoring of the analyte concentrations, operation of the immunosensor with the enzyme conjugate as signal generator required special attention to (a) enzyme stability, (b) analyte permeation (dependence on medium components), and (c) kinetics related to the different accessibility to the same antibody of the small analyte (to be measured) vs. the larger counterpart on the enzyme conjugate (for signal generation). *Biotechnol Bioeng* **56:** 221–231, 1997.
Keywords: immunosensor; continuous monitoring; enzyme stability; rate-limiting factors; mathematical model

INTRODUCTION

Continuous monitoring of particular molecules, which are present in trace amounts and in a complex medium stream (e.g., blood, wastewater, and fermentation broth), can be achieved by using immunosensor (Andrade et al., 1990; Attili and Suleiman, 1984; Hall, 1990). Such sensors use specific antigen–antibody binding reactions that are reversible, dynamic equilibrium processes and require no separation of unbound reagents from the binding complex formed. Utilization of electrode (metal or semiconductor) as solid matrix for antibody immobilization may make the sensor system simple in operation (Tsuji et al., 1990), which is an important feature needed for field tests. In this sensor configuration, enzymes usually serve as signal generator (Aizawa, 1987). Although these sensors open up new opportunities for monitoring analytes, few applications have been mentioned, and the underlying theories for reversible immunosensors are scarcely described.

Previously, we have investigated a technical solution for continuous monitoring by utilizing an enzyme as signal generator (Schramm and Paek, 1992b). Major elements of the sensor are an analyte–enzyme conjugate and two antibodies, specific to the analyte (Ab_1) and to the enzyme (Ab_2), immobilized on different solid matrices (Fig. 1). The reagents are enclosed in a chamber separated by a semipermeable membrane from a medium stream to be analyzed. This membrane allows small molecules (e.g., native analyte), which are carried by the external medium, to pass through while retaining the conjugate. In the absence of native analyte in the external medium, the conjugate can bind to either antibody (i.e., the conjugate is heterobifunctional). An initial state (no external analyte) in which the conjugate binds predominantly to Ab_1 (Fig. 1, left) can be achieved by selecting antibodies with appropriate binding constants or by controlling the concentration ratio of the immobilized antibodies (Paek and Schramm, 1992). Upon introduction of excess native analyte in the medium, the analyte permeates into the sensor chamber and competes with the conjugate for the binding sites of Ab_1. As a result, the conjugate is dissociated from Ab_1 and eventually captured by Ab_2 (final state; Fig. 1, right). This migration of the conjugate shifts the signal from the side with Ab_1 to the other side containing Ab_2. The sensor returns to the initial state when the medium is depleted of the native analyte.

Because this sensor is devised to measure signals from bound conjugate at the two distinct antibody sites, the sig-

Correspondence to: S.-H. Paek

 CCC 0006-3592/97/020221-11

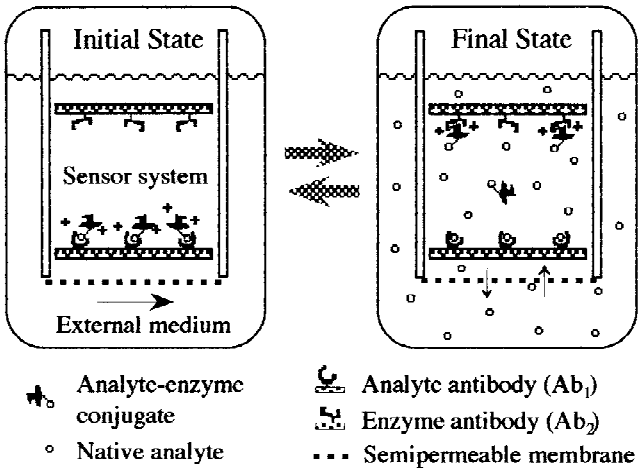

Figure 1. A reversible model system for the continuous monitoring of analyte concentration. At ground (initial) state, an analyte–enzyme conjugate binds predominantly to the analyte antibody (Ab_1). When native analyte is introduced into the external medium, it flows into the sensor chamber across a semipermeable membrane. Competition occurs between the two analyte species for the binding sites of Ab_1. As a result, the conjugate is dissociated from this antibody and eventually is captured by the enzyme antibody (Ab_2; final state). These two states are interchangeable depending on the analyte concentration in the external medium.

nal-to-noise ratio can be controlled by manipulating the binding constants of the antibodies and the amount of each antibody immobilized to minimize the amount of unbound signal generator (the source of the noise). This decrease in noise may allow us to monitor the analyte concentration without separating the bound and free conjugates for signal generation. The concept under investigation may solve some analytical problems (Andrade et al., 1990) but may be subject to limitations related to (a) the stability of enzyme, (b) the integrity of permeability of the membrane over time, and (c) the size of the signal generator.

We have studied these three factors in the described reversible model by experimental and mathematical approaches. In the experimental model, we have used colorimetry to detect the signals from the bound conjugate. However, because the catalytic formation of colored reagents by horseradish peroxidase does not readily permit continuous monitoring, the system has been adapted for semicontinuous monitoring by using discrete determinations to obtain the required measurements. For future applications, we plan to use electrochemical detection with an immunosensor capable of truly continuous monitoring.

MATERIALS AND METHODS

Materials

Horseradish peroxidase (HRP, type VI, 300 units/mg solid; EC 1.11.1.7), 1,5-poly-L-lysine hydrobromide (MW 421,000), and 3,3′,5,5′-tetramethylbenzidine (TMB) were purchased from Sigma (St. Louis, MO). Disuccinimidyl suberate (DSS) and a microdialyzer (system 100) were obtained from Pierce (Rockford, IL). A semipermeable cellulose membrane (molecular weight cutoff 12,000–14,000; flat sheets) and polypropylene monofilament cloth (56.4 mesh counts/in., 250 μm mesh opening, 200 μm thickness, 31% open area) were purchased from Enka (Wuppertal, Germany) and Small Parts Inc. (Miami, FL), respectively. Progesterone-11α-hemisuccinyl-1,5-diaminopentane (P-CAD) was synthesized as described elsewhere (Paek et al., 1993). The following monoclonal antibodies were produced (Schramm and Paek, 1992b): antibody to progesterone (Ab_1, BQ.1), antibody to HRP (Ab_2, 9G9), and antibody to urease for estimating nonspecific binding (NS-Ab).

Substrate for HRP

The substrate solution for HRP contained 10 μL of 3% (v/v) H_2O_2 in water; 100 μL of 10 mg/mL TMB in dimethyl sulfoxide; and 10 mL of 0.05 mol/L acetate buffer, pH 5.1.

Defined Progesterone–HRP Conjugate as Signal Generator

The progesterone derivative, P-CAD, was chemically reacted with the enzyme, HRP, via DSS as a crosslinking reagent (Paek et al., 1993). One progesterone molecule bound to one HRP molecule (P-HRP) was purified on an immunoaffinity column (Paek et al., 1993). P-HRP was diluted with the same volume of 0.01 mol/L phosphate buffer, pH 7.0, containing 0.14 mol/L NaCl, 0.02% (w/v) thimerosal (PBS), and 0.1% (w/v) gelatin (gel-PBS), and stored at 4°C until used.

Immobilized Antibodies On Discs

Polypropylene monofilament mesh discs (4.8 mm diameter) with the following antibodies immobilized on separate discs were prepared: Ab_1 (BQ.1), Ab_2 (9G9), and NS-Ab. The immunoglobulins were immobilized by a modification of the sodium periodate method (Matson and Little, 1988; Sanderson and Wilson, 1971; Schramm and Paek, 1992b). The discs with the immobilized antibodies were stored in gel-PBS at 4°C until used. The surface density of the binding sites of the immobilized antibody was determined by means of Scatchard analyses (Scatchard, 1949; Schramm and Paek, 1991).

Experimental Set-UP for a Reversible Model

The experimental model for the reversible sensor consisted of a microdialyzer with 12 wells (5 × 14 mm, internal compartment; A in Figure 2) and an external medium chamber (B, 100 mL volume). Each well served as a sensor system containing the discs with the immobilized antibodies and the P-HRP conjugate. The wells were separated from the medium chamber by a semipermeable cellulose membrane (C). Medium was supplied to the chamber through tubing

that passes a peristaltic pump and the flow was additionally regulated by valves (D). The medium in the chamber was agitated with a magnetic bar (E). The microdialyzer was placed in a box (F) maintained at 100% humidity and placed on a magnetic stirrer (G). The whole system was then agitated on an orbital shaker (H) to facilitate the mass transfer of molecules within the sensor system.

Determination of HRP Enzymatic Stability

The enzyme activity of HRP in the well (internal compartment, Fig. 2A) of the microdialyzer and in a microtiter well were measured against time. The disc with the immobilized Ab_1 (BQ.1) was placed in each well with 10 μL of 470 fmol/mL P-HRP in a buffer [gel-PBS or gel-PBS containing 1% (w/v) polyethylene glycol (PEG), M_r = 3000–3700 (gel-PBS–PEG); 30 μL total volume]. For the microdialyzer, the same buffer, degassed prior to use, was filled in the external medium chamber and then supplied at the rate of 17 mL/min by a peristaltic pump. After incubating for different time intervals, the discs from each well were washed to eliminate the unbound P-HRP and placed in separate empty microwells. The bound conjugate on the disc was quantified by (a) adding 200 μL of substrate for HRP containing TMB as chromogen, (b) developing color from the oxidized TMB, (c) adding 50 μL of 0.5 mol/L sulfuric acid, (d) measuring the color at A_{450} with a spectrophotometer (microtiter plate reader; Titertek Multiscan, type 310C; Eflab Oy, Finland), and (e) determining the bound P-HRP amount from a standard curve of known concentrations of HRP.

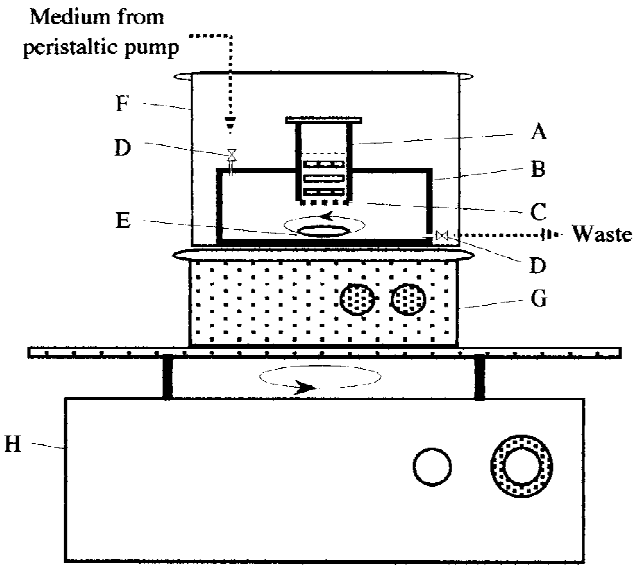

Figure 2. Experimental set-up for continuous monitoring of analytes: A: well in the microdialyzer unit (internal compartment) acting as sensor system that contains the enzyme conjugate and the immobilized antibodies; B: external medium chamber; C: semipermeable membrane; D: one-way valve; E: magnetic bar; F: plastic box maintained at 100% humidity; G: magnetic stirrer; and H: orbital shaker.

Determination of Analyte Permeation Rate Across the Semipermeable Membrane

The permeation rates of analyte (progesterone) across a selected semipermeable membrane were measured in three different buffers: (a) PBS, (b) gel-PBS, and (c) gel-PBS–PEG. The medium chamber of the microdialyzer was filled with buffer, and 100 μL of 10 ng/mL progesterone in the same buffer was added into each well of the dialyzer. The dialyzer was operated as described above. At predetermined times, 50 μL of the progesterone solution in the well was taken as a sample for the determination of the progesterone concentration by a competitive immunoassay.

For the assay, 50 μL of progesterone solution (sample or standard) and 100 μL of 350 fmol/mL P-HRP in gel-PBS (200 μL total volume) were added to a microtiter well with the immobilized Ab_1. This antibody was immobilized on the inner surface of the well by the same procedure used for the disc. After 4 h incubation, the amount of P-HRP bound to the antibody was determined by a colorimetric reaction as mentioned earlier. From the assay with the standard solution of progesterone, a dose–response curve was prepared. The progesterone concentration in the sample was derived from a logit-log transformation of the dose–response curve (Rodbard and Lewald, 1970).

Time–Response Curves from a Reversible Model

To verify the reversibility of the investigated sensor, the response to different progesterone concentrations over time was measured. Each well contained one disc with immobilized Ab_1, two discs with Ab_2, and 10 μL of 470 fmol/mL P-HRP in gel-PBS–PEG (30 μL total volume). The medium chamber was filled with the same buffer. After 3 h of preincubation to reach equilibrium between the conjugate and the two antibodies, 1.25 mL of a 0.8 μg/mL progesterone solution was added to the external buffer chamber to obtain a total concentration of 10 ng/mL (time 0). Starting from this time, P-HRP bound to each antibody on the different discs was measured in intervals by colorimetric detection as described above. After 3 h of incubation, gel-PBS–PEG was supplied to the buffer chamber by a peristaltic pump at a high flow rate (49 mL/min) to decrease the progesterone concentration to less than 0.1 ng/mL in 10 min. The flow rate then decreased to 17 mL/min.

MATHEMATICAL MODEL

To describe the binding reactions at liquid–solid interfaces (Fig. 1), a mathematical model has been developed. The formation of the binding complexes between antigens and antibodies is a result of the following dynamic processes:

(a) association and dissociation reactions of the analytes (native and conjugated to enzyme) with the immobilized antibodies;
(b) diffusion of the analytes between the solid surfaces and

the bulk solution according to the concentration gradients; and

(c) transfer of the native analyte across the semipermeable membrane.

Each of these processes is described by differential equation(s) with respect to time. The formulated equations are used to predict the response of the immunosensor to changes in external analyte concentrations.

Association/Dissociation Reactions of Antigens with Immobilized Antibodies

In the sensor system (Fig. 1), the native analyte and the enzyme conjugate interacts with the two immobilized antibodies. Three different reactions take place: (a) binding of the conjugate with the analyte antibody (Ab_1), (b) the conjugate with the enzyme antibody (Ab_2), and (c) the analyte with Ab_1.

The reaction rates of the conjugate with Ab_1, dC_{x1}/dt, and with Ab_2, dC_{x2}/dt, are expressed based on an assumption that monovalent binding occurs:

$$\frac{dC_{x1}}{dt} = k_{on1}Y_1C_{s1} - k_{off1}C_{x1} \quad (1)$$

$$\frac{dC_{x2}}{dt} = k_{on2}Y_2C_{s2} - k_{off2}C_{x2} \quad (2)$$

where C_x stands for the surface density of the binding complex, Y for the density of the unoccupied binding sites, C_s for the concentration of the conjugate near the solid surface, k_{on} for the association rate constant, and k_{off} for the dissociation rate constant. Subscript 1 represents Ab_1 and subscript 2 Ab_2.

The analyte antibody, Ab_1, also interacts with the analyte, which is much smaller than the analyte–enzyme conjugate. Therefore, as described in previous studies (Schramm and Paek, 1992a), the small analyte can bind to the antigen binding sites of the immobilized antibody, which are inaccessible to the enzyme conjugate due to the steric hindrance of the large enzyme molecule. The binding sites can be divided into two classes: those accessible only to the native analyte ($Y_{1'}$) and those accessible to both the native analyte and the enzyme conjugate (Y_1). The rate constants of the reactions of the small antigen with Y_1 and $Y_{1'}$ are identical.

The formation rates of the binding complexes between the analyte and the two groups of the binding sites, $Y_1(dC_{x3}/dt)$ and $Y_{1'}(dC_{x3'}/dt)$, are

$$\frac{dC_{x3}}{dt} = k_{on3}Y_1P_i - k_{off3}C_{x3} \quad (3)$$

$$\frac{dC_{x3'}}{dt} = k_{on3}Y_{1'}P_i - k_{off3}C_{x3'} \quad (4)$$

where k_{on3} stands for the on-rate constant of the native analyte to Ab_1 and k_{off3} for the off-rate constant. In these two equations, P_i is the concentration of the native analyte in the bulk solution of the system. Since, for this analyte, the diffusion rate is faster than the permeation rate across a semipermeable membrane (see below), the diffusion is not kinetically important in the mathematical modeling. Therefore, P_i can also be used as the surface concentration. Only the diffusion of the enzyme conjugate is considered as a potential rate-limiting process at next section.

Diffusion of Analyte–Enzyme Conjugate

The association/dissociation reactions of the enzyme conjugate with the immobilized antibodies can produce a difference in the conjugate concentration between the area close to the solid surfaces and the bulk solution. This concentration gradient creates a driving force for the diffusion of the antigen species. The diffusion can be facilitated if the medium is agitated. Near the solid surface forms a film, a boundary layer which is not disturbed by the agitation (Trurnit, 1954). The antigen transport through this layer is based on molecular diffusion. Under this condition, rate equations have been previously derived (Paek and Schramm, 1991) for the diffusion of antigens by assuming a linear concentration gradient in the boundary layer and for the subsequent binding reaction with an immobilized antibody.

The rate equation is now expanded for the dual-antibody system. Three concentrations of the conjugate are selected as time-dependent variables: (a) those near the solid surface with Ab_1 (C_{s1}), (b) those near the solid surface with Ab_2 (C_{s2}), and (c) those in the bulk solution (C_b). The conjugates found in C_{s1} and C_{s2} can form binding complexes with the antibodies immobilized on the surface. The rate equations for the changes of C_{s1} and C_{s2} can be derived, as shown previously (Paek and Schramm, 1991), by combining the two material balance equations that describe the rates of change in conjugate concentration in the boundary layer and in bulk solution, assuming a linear concentration gradient across the boundary layer. The rate of change in C_{s1}, dC_{s1}/dt, is described in the equation

$$\frac{dC_{S1}}{dt} = k_c\left(\frac{2}{a} + \frac{S_{h1}}{V - S_t a}\right)(C_b - C_{S1}) + \left(\frac{k_c S_{h2}}{V - S_t a}\right)(C_b - C_{S2}) - \frac{2}{a}r_1\,(k_{on1}\,Y_1C_{S1} - k_{off1}\,C_{X1}) \quad (5)$$

where k_c is the effective mass transfer coefficient for the diffusion of the conjugate and a the thickness of the boundary layer. The term S_h represents the surface area of the boundary layer and S the surface area of the solid matrix. Here, $S_t = S_{h1} + S_{h2}$ and $r_1 = S_1/S_{h1}$, where subscript 1 stands for the solid matrix with Ab_1 and subscript 2 for the solid matrix with Ab_2. On the right-hand side of Equation (5), the first and second terms represent the transport rates of the conjugate at each solid matrix and the third term is the binding reaction rate with Ab_1 [Equation (1)].

A similar rate equation for the change of C_{S2} has been derived:

$$\frac{dC_{S2}}{dt} = \left(\frac{k_c S_{h1}}{V - S_t a}\right)(C_b - C_{S1}) + k_c\left(\frac{2}{a} + \frac{S_{h2}}{V - S_t a}\right)(C_b - C_{S2}) - \frac{2}{a}\, r_2\,(k_{on2}\, Y_2\, C_{S2} - k_{off2}\, C_{X2}) \quad (6)$$

where $r_2 = S_2/S_{h2}$. The third term on the right-hand side represents the binding reaction rate of the conjugate with Ab_2 [Equation (2)].

Transfer of Analyte across a Semipermeable Membrane

Equilibria between the conjugate and the two antibodies are determined by the concentration of analyte from an external medium. When a concentration gradient of the analyte exists between solutions on opposite sides of the semipermeable membrane (Fig. 1), a driving force for the transfer is generated. From a simplified version of Fick's first law of diffusion (Silhavy et al., 1975; Spriggs and Li, 1976), the mass transfer rate can be expressed as $(D_p/w)A(P_o - P_i)$, where D_p is the permeability coefficient, w is the thickness of the membrane, and A is the surface area. The terms P_o and P_i represent the analyte concentrations in the external and internal media, respectively. This equation is most frequently used to describe dialysis assuming (a) a linear analyte concentration profile across the membrane, (b) constant analyte distribution in each medium, and (c) no effect of bulk flow (Silhavy et al., 1975).

It is noted that when P_o and P_i are the bulk concentrations of analyte on either side of the membrane, D_p is not purely the permeability coefficient. To transport from one bulk medium to the other, the analyte molecules have to pass through three layers: the membranes itself and two aqueous films formed near each side of the membrane. Thus, D_p becomes the effective permeability coefficient reflecting the analyte transport through the three layers.

From the conservation law of mass, the accumulation rate of the analyte in the solution of the system (volume V), $(dP_i/dt)V$, is equal to the difference between the permeation rate and the reaction rate with the analyte antibody, $(dC_{x3}/dt + dC_{x3'}/dt)S_1$ [see Equations (3) and (4)]. These terms are combined and rearranged to yield the equation

$$\frac{dP_i}{dt} = k_p\left(\frac{A}{V}\right)(P_0 - P_i) - \frac{S_1}{V}\{k_{on3}\,(Y_1 + Y_{1'})\,P_i - k_{off3}\,(C_{X3} + C_{X3'})\} \quad (7)$$

The first term on the right-hand side of Equation (7) represents the permeation rate of the native analyte and the second the reaction rate with Ab_1.

Supplemental Equations

In the previous sections, seven rate equations were derived for 11 dependent variables [7 variables belong to the left-hand sides in Equations (1)–(7); four variables represent C_b, Y_1, $Y_{1'}$, and Y_2]. Since a solution of the 11 dependent variables requires the corresponding number of equations, four additional equations, (8)–(11), describe the material balance for the conjugate (8), the binding sites of Y_1 (9), the binding sites of $Y_{1'}$ (10), and the binding sites of Y_2 (11):

$$(V - S_t a)C_t = (V - S_t a)C_b + \frac{S_{p1}a}{2}(C_b + C_{S1}) + \frac{S_{p2}a}{2}(C_b + C_{S2}) + S_1 C_{X1} + S_2 C_{X2} \quad (8)$$

$$Y_{t1} = Y_1 + C_{X1} + C_{X3} \quad (9)$$

$$Y_{t1'} = Y_{1'} + C_{X3'} \quad (10)$$

$$Y_{t2} = Y_2 + C_{X2} \quad (11)$$

where subscript t stands for total.

Dimensionless groups

For convenient manipulation and to reduce the number of independent variables, all of the variables in Equations (1)–(11) are normalized. Dependent variables are scaled by total concentraiton of the conjugate, C_t. Independent variables are arranged to form the following dimensionless groups:

$$R_1 = \frac{k_{on1}\, Y_{t1}}{k_c} \qquad R_2 = \frac{k_{on2}\, Y_{t2}}{k_c}$$

$$R_3 = \frac{k_{on3}\,(Y_{t1} + Y_{t1'})}{k_c} \qquad R_4 = \frac{k_{off1}\,\lambda_1}{k_{on1} Y_{t1}}$$

$$R_5 = \frac{k_{off2}\,\lambda_2}{k_{on2} Y_{t2}} \qquad R_6 = \frac{k_{off3}\,\lambda_1}{k_{on3}\,(Y_{t1} + Y_{t1'})}$$

$$R_7 = \frac{k_p}{k_c} \qquad \tau = \left(\frac{k_c}{a}\right) t$$

Using the normalized variables, Equations (1)–(7) are reformulated and then simultaneously solved by a numerical method [e.g., the fourth-order Runge–Kutta method (Romanelli, 1960)].

RESULTS AND DISCUSSION

Stabilization of Enzyme Activity in a Reversible Immunosensor

The enzyme used in the analyte–enzyme conjugate (P-HRP) as signal generator may be sensitive to the components (inhibitors) of the medium that block the catalytic site. Since various enzymes are inactivated by different inhibitors, each enzyme must be investigated separately. The enzymatic stability of the selected enzyme, HRP, in the reversible model has been examined, and a method for the stabilization of the enzyme is presented.

Enzyme Activity in a Reversible Model

The activity of HRP in the chamber of the sensor (microdialyzer, Fig. 2) was compared with HRP activity in a regular microtiter well (Fig. 3). The sensor compartment of the microdialyzer is open to small molecules (MW $\leqslant$ 12,000) via the semipermeable membrane. In contrast, the microwell is a closed system that does not have material exchange. Under the experimental conditions used, the volume passing through the microdialyzer is a million-fold larger (calculated for 24 h operation) than that in the sensor compartment. Therefore, the enzyme can potentially be exposed to a substantial amount of inhibitors.

After 24 h incubation in a microwell, the HRP retained 90% of its original activity even at low concentrations (4.7 fmol/30 μL; Microwells; Gel-PBS in Fig. 3). When the same amount of enzyme was incubated in the microdialyzer, the enzyme lost about 50% of the initial activity (Microdialyzer; Gel-PBS).

The reagents (NaCl, $NaH_2PO_4 \cdot H_2O$, Na_2HPO_4) used for the preparation of PBS and the cellulose semipermeable membrane may contain trace amounts of enzyme inhibitors such as sulfate, sulfide, and heavy metals. Sulfide is known to form stable complexes with the heme of HRP (Dixon and Webb, 1964; Saunders et al., 1964) that is a part of the catalytic site (Ator et al., 1987; Gasyna et al., 1988). Free radicals that can inhibit the enzyme reaction (Ator et al., 1987) might also be present in the buffer.

PEG as Preservative of Enzyme Activity

Addition of 1% (w/v) PEG, M_r = 3000–3700, to the buffer (gel-PBS) was effective in preserving the enzyme activity (Microdialyzer; Gel-PBS-PEG in Fig. 3). During an incubation period of about 24 h, the presence of PEG resulted in 50% increase in the enzyme activity.

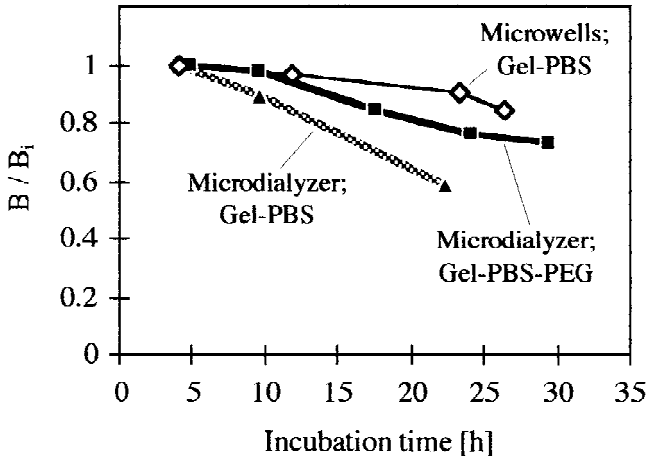

Figure 3. Loss of activity of horseradish peroxidase (HRP) over time. The enzyme activity at time *t* compared to the activity after 4 h incubation (B/B_i) was measured from the progesterone–HRP conjugate (P-HRP) bound to an immobilized progesterone antibody. The inactivation rate of HRP was faster in a well from a microdialyzer (partially open system) than in a well of microtiter plate (closed system). The inactivation rate was reduced in a medium containing polyethylene glycol (PEG).

The polymer, PEG, may affect the enzyme in two ways: (a) by chelating heavy metals (Evdokimov et al., 1975) and (b) by decreasing aggregation of protein molecules (Andersson et al., 1979). A strong chelating agent, such as ethylenediaminetetraacetic acid, cannot be used because it also eliminates Ca^{2+}, which is a cofactor for HRP (Kretsinger, 1976). The deaggregating properties of PEG originate from the large number of ether-linked oxygen atoms that render this polymer hydrophilic and reduce the hydrophobic interactions among protein molecules (Andersson et al., 1979; Tilcock and Fisher, 1982).

Effect of PEG on the Rates of Kinetic Processes

As a medium component, PEG may alter the rates of mass transfer. The hydration of the polymer at high concentrations may increase the medium viscosity, which decreases the diffusion rates of other medium components. Since PEG is randomly coiled, small molecules can diffuse through this structure. This transfer rate depends on the size of the diffusing molecules [sieving effect (Laurent, 1966; Polson, 1977)]. Rates of kinetic processes in a medium containing 1% PEG (gel-PBS–PEG) have been examined.

Permeation of Progesterone

The molecular diffusion of progesterone through the semipermeable membrane, i.e., permeation, could be affected by the presence of PEG. The ratio of the diameter of the membrane pore to the diameter of the PEG molecule (average M_r = 3350) was estimated by using four assumptions: (a) the pore size of the membrane is uniform; (b) the pore size is represented by the maximum dimension (M_r = 12,000) of a molecule that can pass through the membrane; (c) the investigated molecules have globular shape; and (d) the molecular densities are constant. With these assumptions, the diameter ratio of the pore to the PEG molecule is about 1.4. Consequently, the polymer in the medium significantly reduces the free path of the pores for permeation of smaller analytes.

By using the microdialyzer, the permeation rates in three different media were compared (Fig. 4): PBS, gel-PBS, and gel-PBS–PEG. For these experiments, progesterone was added not to the external medium but to the internal compartment of the dialyzer. The decrease (relative to the initial concentration, $P_{i,t=t'}/P_{i,t=0}$) in the internal analyte concentration (P_i) was measured over time. After 4 h, the permeation rate with gel-PBS–PEG was significantly slower than with the other two media.

The permeation rate (dP_i/dt) can be mathematically expressed as $k_p(A/V)(P_o - P_i)$ (see Mathematical Model), where k_p is the effective mass transfer coefficient for permeation, A the surface area of the membrane, V the system volume, P_o the external analyte concentration, and P_i the

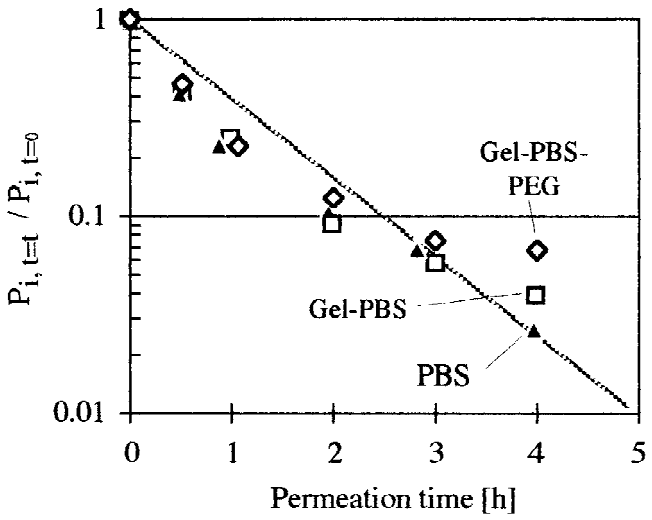

Figure 4. Permeation of progesterone across the semipermeable membrane in different media: PBS, gel-PBS, and gel-PBS–PEG. The decrease in the progesterone concentration by permeation relative to the initial concentration ($P_{i,t=t}/P_{i,t=0}$) was measured over time.

internal concentration. After integration of this equation at $P_o \approx 0$, the following expression is obtained:

$$\log\left(\frac{P_{i,t=t}}{P_{i,t=0}}\right) = -k_p\left(\frac{A}{2.303\,V}\right) t$$

According to this equation, the concentration decrease in the semilog plot can be represented by a straight line with the slope of $-k_p(A/2.303V)$. Although with none of the investigated media was a straight line experimentally obtained, a line using the data points from PBS shown in Figure 4 was constructed to determine k_p for the calculation of theoretical time–response data of the sensor. Thus, relative permeation rates in the three media were compared.

Antigen–Antibody Complex Formation and Molecular Diffusion in Bulk Solution

PEG has been reported to affect the activities of the antigen–antibody reaction (Lizana and Hellsing, 1974) as well as the diffusion rates of other molecules in bulk solution (Polson, 1977). These effects of PEG depend on the polymer concentration. The following three variables were determined in gel-PBS–PEG and compared with those in gel-PBS (Schramm and Paek, 1992b): (a) the association and (b) the dissociation rate constants of the binding reaction between P-HRP and the progesterone antibody (Ab_1) and (c) the mass transfer coefficient for diffusion (diffusion coefficient divided by thickness of penetration layer) of P-HRP. The measured values agreed within 5% for the two different media, and the differences may be attributable to experimental error rather than to medium composition.

It has been shown that the addition of 1% PEG to the sensor medium preserved HRP activity and did not significantly alter the process rates except for the permeation rate of progesterone. In the following experiments, 1% PEG in the medium has been used to obtain response curves to varying concentrations of external analyte.

Response of the Reversible Sensor to Analyte Concentrations

The reversible dual-antibody system has been described in Figure 1 using two major components: (a) P-HRP as heterobifunctional signal generator and (b) the two antibodies [specific to progesterone, P, (Ab_1) and to HRP (Ab_2)]. Since the concentrations of these two components are constant, the only variable that can affect the equilibrium binding between P-HRP and the two antibodies is the analyte concentration. The variation of the bound P-HRP as the sensor response is presented by an expanded mathematical model (see Mathematical Model). The calculations are then compared with experimental results obtained by utilizing gel-PBS–PEG as medium.

Theoretical Time–Response Curves

The different accessibilities of P and P-HRP to the immobilized antibody (Schramm and Paek, 1992a), Ab_1, have been incorporated into the mathematical model. The large antigen P-HRP binds to a smaller number of the antigen binding sites for Ab_1 than does the native progesterone, P (Table I). In the previous calculation (Schramm and Paek, 1992b), only the number of antigen binding sites accessible to P-HRP was considered to describe the formation of antigen–antibody binding complexes [Equations (1) and (3) in Mathematical Model]. Subsequently, the model was updated by including the additional antigen binding sites available only for binding P [Equation (4)].

In Figure 5 (middle panel, phases A–C), the 95% equilibrium of the calculated sensor response to different concentrations of external analyte is shown. The analyte concentration (top panel) was increased from zero (phase A) to 10 ng/mL (phase B) and returned to zero (phase C). The total time for returning to the initial state was about 19 h. This was two times longer than the time previously calculated (Schramm and Paek, 1992b). The slower response with the revised model results from the consideration of the

Table I. Experimentally determined densities of antibody binding sites accessible to different antigen species.

Variable	Symbol	Experimentally determined (fmol/disc)
Density of binding sites on Ab_1		
accessible to P-HRP	Y_{t1}	12
accessible to P[a]	$Y_{t1'}$	360
Density of binding sites on Ab_2		
accessible to P-HRP	Y_{t2}	13

[a]Approximation, determined by using ^{125}I-labeled progesterone (Schramm and Paek, 1991).

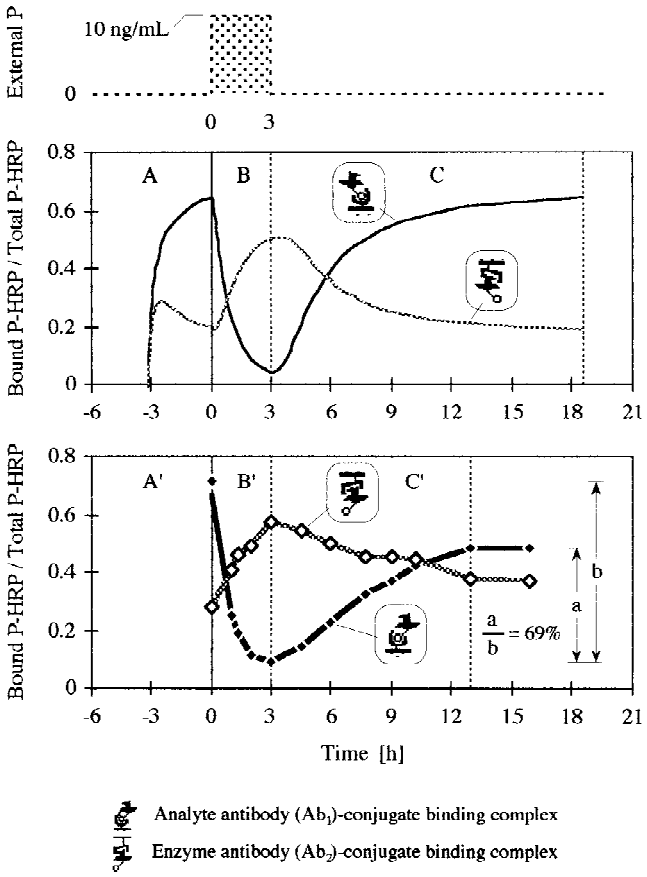

Figure 5. Sensor response to changing analyte concentrations in an external medium (top panel). The response curves derived from mathematical modeling (middle panel) are compared to those experimentally obtained (bottom panel). The theoretical curves were calculated based on 95% equilibrium of antigen–antibody complex formation. The time required for returning to the original state (time 0) was about 19 h. In the experiment, the equilibrium did not completely return to the initial state. Only 69% of the complex formation at time 0 was obtained after about 10 h following the withdrawal of progesterone.

excess antibody binding sites for P. Rate-limiting factors for the response time are identified in the next section.

Experimental Time–Response Curves

The experimental conditions described in this investigation were the same as previously reported (Schramm and Paek, 1992b) except for the use of (a) gel-PBS containing 1% PEG as medium, (b) the concentration of the external analyte, (c) discs with two times larger mesh size, and (d) different ratio of the two antibody concentrations. With 10 ng/mL of progesterone, the minimal analyte concentration in the external medium that is required to reach the final state (Fig. 1, right) was selected. Discs with larger mesh size were used to diminish potential mass transfer limitations of the conjugate between the solid surface and the bulk solution. Since the discs were also thicker, the number of discs with immobilized HRP antibody that can be placed in addition to one disc with the progesterone antibody in a sensor chamber was limited. This caused a different ratio of the two antibody concentrations from that previously used.

The experimental response curves (Fig. 5, bottom panel) obtained under these conditions were compared with those in the previous report (Schramm and Paek, 1992b). In both experiments, the curves did not return to the initial state. However, incomplete recoveries could have at least partially different reasons. In the absence of PEG, the enzyme HRP has been shown to be inactivated faster than in the presence of PEG (Fig. 3). This could be the reason for the low recovery in the earlier experiment. Although enzyme inactivation is decreased in the presence of PEG, this advantage is counteracted by a slower permeation of analyte across the semipermeable membrane (Fig. 4). This may result in a residue of analyte within the system that can also cause an incomplete return to the initial state (Fig. 5, bottom panel). As a result, the experimental results shown in Figure 5 and in the previous study were similar but for different reasons. Further, optimization of a sensor system based on these results will be subject of later investigations.

In the next section, steps that are rate limiting for the sensor response were quantified by using the algorithms developed in Mathematical Model. Since the analyte itself does not provide a readily measurable signal, mathematical calculations have been used to trace the analyte behavior in the sensor system.

Identification of Rate-Limiting Factors

Kinetic Model

The different equilibrium reactions of the sensor are sequential kinetic processes. One or more of these steps may be rate limiting for the response. The processes have been characterized (Fig. 6) by using dimensionless groups (R_1 to R_7 in Mathematical Model). Each of the groups represent the ratio of two kinetic processes. Here, R_1 to R_3 are the ratios of the association reactions of the two antigens with the antibodies

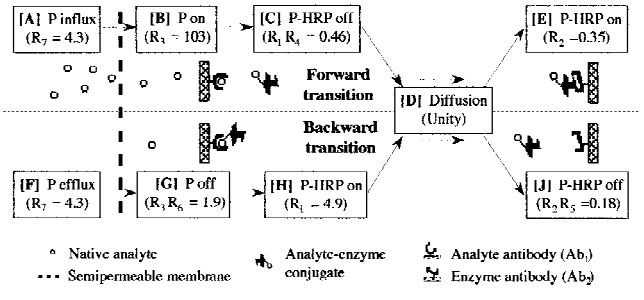

Figure 6. The sequences of kinetic processes which affect sensor responses to the increase (forward transition) and the decrease (backward transition) of external analyte concentration. The rate of each process was normalized to the rate of P-HRP diffusion (values in parentheses) by appropriately combining the dimensionless groups (R_1 to R_7) derived in Mathematical Model. This permitted to compare the normalized rates with each other. The terms R_1 to R_7 were calculated by using the values shown in Table I and presented elsewhere (Schramm and Paek, 1992b).

and the diffusion of the conjugate, respectively; R_4 to R_6 are for the dissociation reactions and the association reactions between the antigens and the antibodies; and R_7 stands for the permeation of the analyte and the diffusion of the conjugate.

The dimensionless groups were combined such that each process was normalized to the rate of P-HRP diffusion (Fig. 6). This procedure allows to compare the normalized rates with each other. For example, process A (influx of P) is 4.3 times faster than process D (diffusion of P-HRP).

As the external analyte concentration is increased, processes A–E (Fig. 6, upper panel) shift the sensor from the initial state to the final state (Fig. 5B; forward transition). By comparing the normalized rates, the potential rate-limiting steps in this transition was E followed by C, i.e., the association of P-HRP with the enzyme antibody (Ab_2) and the dissociation of P-HRP bound to the analyte antibody (Ab_1), respectively.

The backward transition (Fig. 5C) consists of processes F–J (Fig. 6, lower panel). Here, the counterpart processes of the forward transition are shown. In the backward transition, the dissociation of P-HRP bound to Ab_2 (Fig. 6J) was by far the slowest process, i.e., about half of the rate-limiting process of the forward transition (Fig. 6J vs. 6E).

From this analysis, one can predict that the response time of the sensor in the backward transition is two times slower than in the forward transition. However, there is a discrepancy between this model and the calculated response curves that shows a backward transition which is five times slower (Fig. 5C). This will be examined in the next section.

Potential Reassociation

At the liquid–solid interface, the dissociating antigen has the potential to reassociate with the immobilized antibody. In the backward transition, the decrease in the binding complex density by dissociation (Fig. 7C, dashed curve) is much slower than the decrease in the internal concentration of P (solid curve) if we consider solely permeation. During the initial period of analyte efflux, the dissociation occurs at maximal rates, and some unoccupied binding sites of the antibody are produced. As the dissociation process further continues, there is an increasing probability that the dissociating P will reassociate with the increasing number of unoccupied binding sites at Ab_1 (Berzofsky and Berkower, 1984; Stenberg et al., 1988). Reassociation is directly proportional to the ratio ($R_3/R_7 = 24$) of the rates of association ($R_3 = 103$, Fig. 6B) and permeation ($R_7 = 4.3$; Fig. 6F) (Silhavy et al., 1975). (Note that the permeation is a slower process than the diffusion of P. Therefore, diffusion can be ignored.) The fast association rate (and, as a result, slow dissociation rate) is caused by the high surface density (Table I) of the antibody binding sites which is, therefore, responsible for the slow response time of the sensor (Fig. 5C).

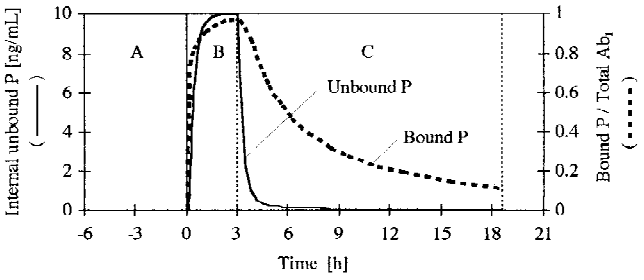

Figure 7. Concentration variations of internal unbound analyte P (solid curve, left axis) and the bound to immobilized Ab_1 at different concentrations of external analyte. The concentration of the binding complex was normalized to total antibody binding sites available for P (dashed curve, right axis). Phases A to C are equivalent to those in the middle panel of Figure 5.

To verify the surface density effect on the response time, we select a boundary case in which all binding sites on Ab_1 are equally available to P and P-HRP, i.e., $Y_{t1'} = Y_{t1} = 12$ fmol/disc from Table I and, thus, $Y_{1'} = C_{x3'} = 0$ in Equation (4). Under this condition, the association of P becomes a slower process ($R_3 = 3.4$, which replaces the value of R_3 in Fig. 6B) than the permeation ($R_7 = 4.3$; Fig. 6F). Based on theoretical time–response curves, the response of the sensor in the backward transition takes approximately 2 times longer than that in the forward transition. This is consistent with the earlier prediction made by comparing relative rates of each kinetic processes.

Based on the analyses of the immunosensor above, two questions arise: (1) What is the span of analytes that can be measured with a response time of hours? (2) How long can the sensor be used in a field condition? Although the response is relatively slow, such sensors become increasingly useful for analytes of which concentrations do not fluctuate in a short period of time. Biotechnology products (e.g., antibiotics) for bioprocess control, insecticides and herbicides for environmental monitoring, and toxic compounds (e.g., carcinogens) in waste- and fresh water belong to the analyte range of expectation. However, the test media may contain a variety of substances that affect the sensor stability. Especially, organic solvents, heavy metals, free radicals, and proteolytic activities can cause a conformational change of protein and thus a denaturation. In addition, enzyme reactions for signal generation within the sensor compartment may result in a change of local environment. With an enzyme of glucose oxidase, for instance, the pH of the solution decreases as a result of the catalytic reaction, which affects antigen–antibody binding as well as protein stability. In future investigations, all of these effects will be identified under given conditions, which will then allow to determine the life time of the sensor.

CONCLUSIONS

This research has provided the theoretical and experimental basis for further investigations on the new concept of a dual-antibody sensor that uses a heterobifunctional conjugate as signal generator. Several areas of improvement have

been identified for optimizing the sensor for continuous monitoring. First, it is crucial to select an appropriate enzyme (e.g., glucose oxidase) as signal generator that is stable over time and resistant to medium components which block catalytic sites. The use of a stable enzyme does not only extend the life time of the sensor but also increases the recovery of the ground state since the addition of a stabilizer becomes unnecessary. Second, an enhanced response of the sensor can be achieved by controlled immobilization of antibody. Since different complex formations of the analyte and the conjugate with the immobilized antibody resulted in a slow response time, the antigen binding sites on the antibody must be made equally accessible to small and large antigens. Finally, the response rate can be further enhanced by increasing the dissociation rate constant between antigen and antibody. This can be achieved by a high incubation temperature (Andrade et al., 1990) or an acidic pH of medium, provided that the enzyme as signal generator is stable under these conditions.

We thank Richard H. Smith and Paul A. Craig for critical discussions.

NOMENCLATURE

a	thickness of boundary level (L)
A	surface area of a semipermeable membrane (L^2)
C	concentration of analyte–enzyme conjugate (M/L^3)
$C_{s1,2}$	concentrations of conjugate near solid surface; subscript 1 stands for the surface with analyte antibody and 2 for the surface with enzyme antibody (M/L^3)
$C_{x1,2,3,3'}$	surface densities of binding complexes; subscript 1 for conjugate–analyte antibody complex, 2 for conjugate–enzyme antibody complex, 3 for native analyte–analyte antibody of which binding sites are accessible to both conjugate and analyte, and 3′ for native analyte–analyte antibody of which binding sites accessible only to the analyte (M/L^2)
$k_{off1,2,3}$	dissociation rate constants; see C_x for subscripts 1, 2, and 3 (t^{-1})
$k_{on1,2,3}$	association rate constants; see C_x for subscripts 1, 2, and 3 (L^3/Mt)
k_c, k_p	mass transfer coefficients for diffusion and permeation (L/t)
P_i, P_o	concentrations of native analyte within the sensor compartment and an external medium (M/L^3)
R_{1-7}	dimensionless groups; see Mathematical Model for subscripts 1–7
$r_{1,2}$	surface area ratio of solid matrix to boundary layer; see C_s for subscripts 1 and 2 (dimensionless)
$S_{h1,2}$	surface area of boundary layer near the solid matrix; see C_s for subscripts 1 and 2 (L^2)
S_t	$S_{h1} + S_{h2}$
$S_{1,2}$	surface area of solid matrix; see C_s for subscripts 1 and 2 (L^2)
t	time (t)
V	volume of the system (L^3)
$Y_{1,1',2}$	surface densities of antibody binding sites; subscript 1 for the binding sites on analyte antibody which are accessible to both analyte and conjugate, 1′ for those on the analyte antibody which are accessible only to analyte, and 2 for those on the enzyme antibody (M/L^2)

Greek letters

λ	V_b/S (L)
τ	dimensionless time, $(k_c/a)t$

Subscripts

b	concentration in bulk solution
t	total concentration (bound and unbound)

References

Aizawa, M. 1987. Immunosensors. Phil. Trans. Roy. Soc. Lond. B. **316**: 121–134.

Andersson, K. K., Benyamin, Y., Douzou, P., Balny, C. 1979. The effects of organic solvents and temperature on the desorption of yeast 3-phosphoglycerate kinase from immunosorbent. J. Immunol. Meth. **25**: 375–381.

Andrade, J. D., Lin, J. N., Hlady, V., Herron, J., Christensen, D., Kopecek, J. 1990. Immunosensors: Remaining problems in the development of remote, continuous, multichannel devices, pp. 219–239. In: R. P. Buck, W. E. Hatfield, M. Umana, and E. F. Bowden (eds.), Biosensor technology. Marcel Dekker, New York.

Ator, M. A., David, S. K., de Montellano, P. R. O. 1987. Structure and catalytic mechanism of horseradish peroxidase. J. Biol. Chem. **262**: 14954–14960.

Attili, B. S., Suleiman, A. A. 1995. A piezoelectric immunosensor for the detection of cortisol. Anal. Lett. **28**: 2149–2159.

Berzofsky, J. A., Berkower, I. J. 1984. Antigen-antibody interaction, pp. 595–608. In: W. E. Paul (ed.), Fundamental immunology. Raven Press, New York.

Dixon, M., Webb, E. C. 1964. Enzymes. Academic, New York.

Evdokimov, I., Salianov, V. I., Varshavskii, I. 1975. A compact form of DNA in solution. III. Influence of the ion composition of the solution on the compactization process of double-stranded DNA in the presence of PEG. Molekul. Biol. **9**: 563–573.

Gasyna, Z., Browett, W. R., Stillman, M. J. 1988. Low-temperature magnetic circular dichroism studies of the photoreaction of horseradish peroxidase compound I. Biochemistry. **27**: 2503–2509.

Hall, E. A. H. 1990. Biosensors. Open University Press, Milton Keynes.

Kretsinger, R. H. 1976. Calcium-binding proteins. Ann. Rev. Biochem. **45**: 239–266.

Laurent, T. C. 1966. In vitro studies on the transport of macromolecules through the connective tissue. Fed. Proc. **25**: 1128–1134.

Lizana, J., Hellsing, K. 1974. Manual immunonephelometric assay of proteins, with use of polymer enhancement. Clin. Chem. **20**: 1181–1186.

Matson, R. S., Little, M. C. 1988. Strategy for the immobilization of monoclonal antibodies on solid-phase supports. J. Chromat. **458**: 67–77.

Paek, S. H., Schramm, W. 1991. Modeling of immunosensors under nonequilibrium conditions. Part 1: Mathematic modeling of performance characteristics. Anal. Biochem. **196**: 319–325.

Paek, S. H., Schramm, W. 1992. Irreversible enzyme-shuttle immunoassay. Biotechnol. Bioeng. **39**: 753–764.

Paek, S. H., Bachas, L. G., Schramm, W. 1993. Defined analyte-enzyme conjugates as signal generators in immunoassays. Anal. Biochem. **210**: 145–154.

Polson, A. 1977. A theory for the displacement of proteins and viruses with polyethylene glycol. Prep. Biochem. **7**: 129–154.

Rodbard, D., Lewald, J. E. 1970. Computer analysis of radioligand assay and radioimmunoassay data. Acta Endocrinol. **64**(Suppl. 147): 79–103.

Romanelli, M. J. 1960. Runge-Kutta methods for the solution of ordinary differential equations, pp. 110–120. In: A. Ralston and H. S. Wilf (eds.), Mathematical methods for digital computers. Wiley, New York.

Sanderson, C. J., Wilson, D. V. 1971. A simple method for coupling proteins to insoluble polysaccharides. Immunology **20**: 1061–1065.

Saunders, B. C., Holmes-Siedle, A. G., Stark, B. P. 1964. Peroxidase. The properties and use of a versatile enzyme and of some related catalysts. Butterworth, Washington.

Scatchard, G. 1949. The attractions of proteins for small molecules and ions. Ann. N. Y. Acad. Sci. **51**: 660–672.

Schramm, W., Paek, S. H. 1991. Modeling of immunosensors under non-equilibrium conditions. Part 2: Experimental determination of performance characteristics. Anal. Biochem. **196**: 326–336.

Schramm, W., Paek, S. H. 1992a. Antibody-antigen complex formation with immobilized immunoglobulins. Anal. Biochem. **205**: 47–56.

Schramm, W., Paek, S. H. 1992b. Continuous monitoring of analyte concentrations. Biosensor. Bioelect. **7**: 103–114.

Silhavy, T. J., Szmelcman, S., Boos, W., Schwartz, M. 1975. On the significance of the retention of ligand by protein. Proc. Nat. Acad. Sci. USA **72**: 2120–2124.

Spriggs, H. D., Li, N. H. 1976. Liquid permeation through polymeric membranes, pp. 39–79. In: P. Meares (ed.), Membrane separation process. Elsevier Scientific, New York.

Stenberg, M., Werthen, M., Theander, S., Nygren, H. 1988. A diffusion limited reaction theory for a microtiter plate assay. J. Immunol. Meth. **112**: 23–29.

Tilcock, C. P. S., Fisher, D. 1982. The interaction of phospholipid membranes with poly(ethylene glycol) vesicle aggregation and lipid exchange. Biochim. Biophys. Acta. **688**: 645–652.

Trurnit, H. J. 1954. Studies on enzyme systems at a solid–liquid interface: II. The kinetics of adsorption and reaction. Arch. Biochem. **51**: 176–199.

Tsuji, I., Eguchi, H., Yasukouchi, K., Unoki, M., Taniguchi, I. 1990. Enzyme immunosensors based on electropolymerized polytyramine modified electrodes. Biosens. Bioelect. **5**: 87–101.